Theoretical study of the suppression of thermal background in the Raman-enhanced nondegenerate four-wave-mixing spectrum by a time-delayed method

Panming Fu, Zuhe Yu, Xin Mi, Qian Jiang, and Zhiguo Zhang
Institute of Physics, Chinese Academy of Sciences, P.O. Box 603, Beijing 100 080, China
(Received 18 December 1991)

We have studied theoretically the dependence of the Raman-enhanced nondegenerate four-wave-mixing (RENFWM) spectrum on the relative time delay between two pump beams τ when a thermal effect exists in the sample. Using the chaotic model for the incident laser beams, we give the conditions that the thermal background can be eliminated completely when the relative time delay is much longer than the laser coherence time. In this limit, the theoretical RENFWM spectra show the normal asymmetry due to the interference between the Raman-resonant term and the nonresonant background originating solely from the molecular-reorientational grating. We then turn our attention to the dependence of the RENFWM signal intensity on the relative time delay when the laser frequencies are fixed. Our results indicate that RENFWM is asymmetric about $\tau=0$ and the maximum of the RENFWM signal does not occur at $\tau=0$. When the beating frequency between the pump beam and the probe beam is off resonant from the Raman mode, the RENFWM signal exhibits damping oscillation as the time delay increases. We also show that the temporal behavior of the RENFWM signal is drastically different if the laser sources are described by a phase-diffusion model. The different roles of the phase fluctuation and the amplitude fluctuation can be understood in the time domain.

PACS number(s): 42.65.Dr, 42.65.Hw

I. INTRODUCTION

Coherent Raman spectroscopy [1,2] has become a powerful tool for studying the vibrational or rotational mode of a molecule. The most commonly used coherent Raman spectroscopy is coherent anti-Stokes Raman scattering (CARS) [3] and Raman-induced Kerr-effect spectroscopy (RIKES) [4]. Recently, we have made a detailed study of Raman-enhanced nondegenerate four-wave mixing (RENFWM) [5] and demonstrated that it has the features of nonresonant background suppression, free choice of interaction volume, and simple optical alignment. It can also provide excellent spatial signal resolution even for the case of a small dispersion and small Raman shifts, as in the case of pure rotational Raman scattering.

RENFWM is a third-order nonlinear-optical effect with its signal intensity proportional to the absolute square of the third-order nonlinear susceptibility $|\chi^{(3)}_{ijkl}|^2$. $\chi^{(3)}_{ijkl}$ can be decomposed into a Raman-resonant part χ^{R}_{ijkl} and a nonresonant part χ^{NR}_{ijkl}. The RENFWM spectrum appears asymmetric due to the interference between the nonresonant background and the Raman-resonant term. In RENFWM experiment, χ^{NR}_{ijkl} originates mainly from the molecular-reorientational grating formed by the interference of two pump beams. If we know χ^{R}_{ijkl} from other technique such as conventional Raman scattering, the third-order nonlinear susceptibility due to the molecular reorientation can be deduced from the RENFWM spectrum. Now, let us consider a sample which can absorb light at the frequency of the pump beams. In this case, the absorption of the interferent field between two pump beams and subsequently nonradiative decay give rise to a thermal grating of temperature variation [6]. In other words, both the molecular reorientation and the thermal effect contribute to the nonresonant part of the RENFWM signal. One way to eliminate the thermal effect is to use the cross polarization of two pump beams. We can obtain the tensor component χ^{NR}_{1221} or χ^{NR}_{1212} of the third-order nonlinear susceptibility by this polarization configuration.

Recently, we proposed a time-delayed method to distinguish the molecular-reorientational grating from the thermal grating [7]. This method employs the intrinsic incoherence of pump beams and the order-of-magnitude difference between the relaxation time of the molecular-reorientational grating and the thermal grating. The tensor component χ^{NR}_{1111} originating from the molecular reorientation can be measured by this method. The first experiment was performed in a dye-dissolving benzene [8]. By measuring the time-delayed dependence of the RENFWM spectrum, we demonstrated that the thermal grating could be eliminated when the relative time delay was much longer than the laser coherence time τ_c. However, our experimental results showed that there was a distortion of the RENFWM spectrum. Specifically, the interference between the nonresonant background and the Raman-resonant term disappears almost completely. The physical origin of this distortion is unclear. The purpose of this paper is to study theoretically the dependence of the RENFWM spectrum on the relative time delay τ between two pump beams when the thermal effect exists in the sample. We assume that the incident laser beams are chaotic field. We also neglect the saturation effect and restrict our investigations to a pure third-order nonlinear process. Our calculation indicates that under cer-

tain conditions the thermal background can be eliminated completely when the relative time delay is much longer than the laser coherence time. Furthermore, the theoretical RENFWM spectra show the normal asymmetry due to the interference between χ^{R}_{1111} and χ^{NR}_{1111}.

Another problem is the dependence of the RENFWM signal intensity on the relative time delay between two pump beams when the frequencies of the incident beams are fixed. This problem is interesting particularly for the case that the laser coherence time is much shorter than the relaxation time of the material, therefore the laser source can be regarded as an incoherent light. Recently, Morita and Yajima [9] proposed a time-delayed four-wave mixing (FWM) with incoherent light in a two-level system to achieve ultrafast temporal resolution of a relaxation process. This technique has been applied to measure the relaxation time in Nd glass [10], atomic vapor [11], and dye solution [12,13]. In an inhomogeneous broadened system, these experiments show basically a photon echo phenomenon. Hattori, Terasaki, and Kobayashi [14] extended this method to a three-level system. They studied the dephasing time of a Raman vibrational mode by a time-delayed coherent Stokes Raman scattering (CSRS) with incoherent light. Physically, the time-delayed RENFWM with incoherent light is similar to the corresponding CSRS. On the other hand, unlike the CSRS with incoherent light [14], the time-delay dependence of RENFWM is asymmetric about $\tau=0$ and the maximum of the RENFWM signal does not occur at $\tau=0$. When the beating frequency between the pump beam and the probe beam is off resonant from the Raman mode, the RENFWM signal exhibits damping oscillation as the time delay increases. We also study the temporal behavior of the RENFWM signal if the laser sources are described by a phase-diffusion model [15,16], where the laser amplitude is a constant while its phase fluctuates as a random variable. Considering the Raman term only, our result indicates that RENFWM is independent of the relative time delay, which is drastically different from the result based on a chaotic model. Finally, the different roles of the phase fluctuation and the amplitude fluctuation in the time-delayed RENFWM can be understood by a time-domain picture.

The paper is organized as follows. In Sec. II we derive equations which describe the dependence of the RENFWM signal intensity on the frequency detuning for Raman resonance and the relative time delay between two pump beams. Section III is devoted to the theoretical study of the suppression of the thermal background in the RENFWM spectrum. In Sec. IV we study the time-delay dependence of the RENFWM signal for different laser linewidth and frequency detuning when the frequencies of the incident beams are fixed. The different roles of the phase fluctuation and the amplitude fluctuation have also been discussed in this section.

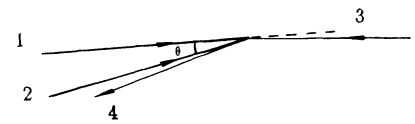

FIG. 1. Schematic diagram of the geometry of Raman-enhanced nondegenerate four-wave mixing.

II. BASIC THEORY

The basic geometry of RENFWM is shown in Fig. 1. Beams 1 and 2 used as pump beams have the same frequency ω_1 and a small angle θ exists between them. The probe beam (beam 3) and the signal (beam 4) with the same frequency ω_3, are almost propagating along the direction opposite to that of beams 1 and 2, respectively. In an absorbing liquid, the interaction of two pump beams gives rise to a molecular-reorientational grating and a thermal grating. On the other hand, when $|\omega_1-\omega_3|$ is near the Raman frequency ω_R, a moving grating formed by the interference of beams 2 and 3 will excite the Raman-active vibrational mode of the material and enhance the FWM signal. The complex incident laser fields can be written as

$$E_i(\mathbf{r},t)=A_i(\mathbf{r},t)\exp(-i\omega_i t)$$
$$=\varepsilon_i u_i(t)\exp[i(\mathbf{k}_i\cdot\mathbf{r}-\omega_i t)] \quad (i=1,2,3)\,, \tag{1}$$

where $A_i(\mathbf{r},t)=\varepsilon_i u_i(t)\exp(i\mathbf{k}_i\cdot\mathbf{r})$. ε_i and $\mathbf{k}_i$ are the constant field magnitude and the wave vector of the ith beam, respectively. $u_i(t)$ is a dimensionless statistical factor that contains the phase and the amplitude fluctuations.

In Appendix A we derive the induced polarization originating from the molecular-reorientational grating, the thermal grating, and the Raman-active mode. From Eqs. (A3), (A6), and (A9), we have the total polarization

$$P(\mathbf{r},t)=P_M(\mathbf{r},t)+P_T(\mathbf{r},t)+P_R(\mathbf{r},t)$$
$$=\varepsilon_1\varepsilon_2^*\varepsilon_3\exp i[(\mathbf{k}_1-\mathbf{k}_2+\mathbf{k}_3)\cdot\mathbf{r}-\omega_3 t]$$
$$\times\left[\chi_M\gamma_M\int_0^\infty dt' u_1(t-t')u_2^*(t-t')u_3(t)\exp(-\gamma_M t')+\chi_T\gamma_T\int_0^\infty dt' u_1(t-t')u_2^*(t-t')u_3(t)\exp(-\gamma_T t')\right.$$
$$\left.+i\chi_R\gamma_R\int_0^\infty dt' u_1(t)u_2^*(t-t')u_3(t-t')\exp[-(\gamma_R-i\Delta)t']\right]. \tag{2}$$

In our case, beams 1 and 2 come from a single laser source. Letting τ be the time delay of beam 1 with respect to beam 2, we have $u_1(t)=u(t-\tau)$, $u_2(t)=u(t)$. The FWM signal is proportional to the average of the absolute square of the polarization over the random variable of the stochastic process. We have

$$
\begin{aligned}
I(\Delta,\tau) \propto\ & (\chi_M\gamma_M)^2\int_0^\infty ds'\int_0^\infty dt'\langle u(t-t'-\tau)u(t-s')u^*(t-s'-\tau)u^*(t-t')\rangle\langle u_3(t)u_3^*(t)\rangle\exp[-\gamma_M(t'+s')] \\
& +(\chi_T\gamma_T)^2\int_0^\infty ds'\int_0^\infty dt'\langle u(t-t'-\tau)u(t-s')u^*(t-s'-\tau)u^*(t-t')\rangle\langle u_3(t)u_3^*(t)\rangle\exp[-\gamma_T(t'+s')] \\
& +(\chi_R\gamma_R)^2\int_0^\infty ds'\int_0^\infty dt'\langle u(t-\tau)u(t-s')u^*(t-\tau)u^*(t-t')\rangle \\
& \qquad \times\langle u_3(t-t')u_3^*(t-s')\rangle\exp[i\Delta(t'-s')]\exp[-\gamma_R(t'+s')] \\
& +\chi_M\chi_T\gamma_M\gamma_T\left[\int_0^\infty ds'\int_0^\infty dt'\langle u(t-t'-\tau)u(t-s')u^*(t-s'-\tau)u^*(t-t')\rangle\langle u_3(t)u_3^*(t)\rangle\exp[-(\gamma_M t'+\gamma_T s')]\right. \\
& \qquad \left.+\int_0^\infty ds'\int_0^\infty dt'\langle u(t-t'-\tau)u(t-s')u^*(t-s'-\tau)u^*(t-t')\rangle\langle u_3(t)u_3^*(t)\rangle\exp[-(\gamma_T t'+\gamma_M s')]\right] \\
& +i\chi_M\chi_R\gamma_M\gamma_R\left[\int_0^\infty ds'\int_0^\infty dt'\langle u(t-\tau)u(t-s')u^*(t-s'-\tau)u^*(t-t')\rangle\right. \\
& \qquad \times\langle u_3(t-t')u_3^*(t)\rangle\exp(i\Delta t')\exp[-(\gamma_R t'+\gamma_M s')] \\
& \qquad -\int_0^\infty ds'\int_0^\infty dt'\langle u(t-t'-\tau)u(t-s')u^*(t-\tau)u^*(t-t')\rangle \\
& \qquad \left.\times\langle u_3(t)u_3^*(t-s')\rangle\exp(-i\Delta s')\exp[-(\gamma_M t'+\gamma_R s')]\right] \\
& +i\chi_T\chi_R\gamma_T\gamma_R\left[\int_0^\infty ds'\int_0^\infty dt'\langle u(t-\tau)u(t-s')u^*(t-s'-\tau)u^*(t-t')\rangle\right. \\
& \qquad \times\langle u_3(t-t')u_3^*(t)\rangle\exp(i\Delta t')\exp[-(\gamma_R t'+\gamma_T s')] \\
& \qquad -\int_0^\infty ds'\int_0^\infty dt'\langle u(t-t'-\tau)u(t-s')u^*(t-\tau)u^*(t-t')\rangle \\
& \qquad \left.\times\langle u_3(t)u_3^*(t-s')\rangle\exp(-i\Delta s')\exp[-(\gamma_T t'+\gamma_R s')]\right] . \qquad (3)
\end{aligned}
$$

We assume that the pump laser is a multimode thermal source. In this case, $u(t)$ has Gaussian statistics with its fourth-order coherence function satisfying [17]

$$\langle u(t_1)u(t_2)u^*(t_3)u^*(t_4)\rangle=\langle u(t_1)u^*(t_3)\rangle\langle u(t_2)u^*(t_4)\rangle+\langle u(t_1)u^*(t_4)\rangle\langle u(t_2)u^*(t_3)\rangle\ . \qquad (4)$$

If the laser sources have Lorentzian line shape, we have the second-order coherence function

$$\langle u(t)u^*(t-\tau)\rangle=\exp(-\alpha|\tau|)\ , \qquad (5)$$

$$\langle u_3(t)u_3^*(t-\tau)\rangle=\exp(-\alpha_3|\tau|)\ . \qquad (6)$$

Here $\alpha=\delta\omega_1/2$, $\alpha_3=\delta\omega_3/2$ with $\delta\omega_1$ and $\delta\omega_3$ the laser linewidth [full width at half maximum (FWHM)] of beams 1 and 3. Substituting Eqs. (4)–(6) into Eq. (3) and performing all the integrals, we obtain, for (i) $\tau>0$,

$$
\begin{aligned}
I(\Delta,\tau)\propto{}&\chi_M^2\left[\frac{\gamma_M}{\gamma_M+2\alpha}\right]+\chi_T^2\left[\frac{\gamma_T}{\gamma_T+2\alpha}\right]+\chi_R^2\left[\frac{\gamma_R(\gamma_R+\alpha+\alpha_3)}{(\gamma_R+\alpha+\alpha_3)^2+\Delta^2}\right]+2\chi_M\chi_T\left[\frac{\gamma_M\gamma_T(\gamma_M+\gamma_T+4\alpha)}{(\gamma_M+\gamma_T)(\gamma_M+2\alpha)(\gamma_T+2\alpha)}\right]\\
&-2\chi_M\chi_R\left[\frac{\gamma_M\gamma_R\Delta}{(\gamma_M+\gamma_R+\alpha+\alpha_3)^2+\Delta^2}\right]\left[\frac{\gamma_M+2(\gamma_R+\alpha+\alpha_3)}{(\gamma_R+\alpha+\alpha_3)^2+\Delta^2}+\frac{1}{\gamma_M+2\alpha}\right]\\
&-2\chi_T\chi_R\left[\frac{\gamma_T\gamma_R\Delta}{(\gamma_T+\gamma_R+\alpha+\alpha_3)^2+\Delta^2}\right]\left[\frac{\gamma_T+2(\gamma_R+\alpha+\alpha_3)}{(\gamma_R+\alpha+\alpha_3)^2+\Delta^2}+\frac{1}{\gamma_T+2\alpha}\right]\\
&+\exp(-2\alpha|\tau|)\left[\chi_M^2+\chi_T^2+\chi_R^2\left[\frac{\gamma_R^2(\gamma_R-\alpha+\alpha_3)}{(\gamma_R-\alpha)[(\gamma_R-\alpha+\alpha_3)^2+\Delta^2]}\right]\right.\\
&\qquad\left.+2\chi_M\chi_T-2\chi_R(\chi_M+\chi_T)\left[\frac{\gamma_R\Delta}{(\gamma_R-\alpha+\alpha_3)^2+\Delta^2}\right]\right]\\
&+\chi_R^2\gamma_R^2\exp(-2\gamma_R|\tau|)\left[\frac{\gamma_R-\alpha-\alpha_3}{(\gamma_R-\alpha)[(\gamma_R-\alpha-\alpha_3)^2+\Delta^2]}+\frac{\gamma_R+\alpha+\alpha_3}{(\gamma_R+\alpha)[(\gamma_R+\alpha+\alpha_3)^2+\Delta^2]}\right.\\
&\qquad\left.-\frac{2[\gamma_R^2+\Delta^2-(\alpha+\alpha_3)^2]}{[(\gamma_R+\alpha+\alpha_3)^2+\Delta^2][(\gamma_R-\alpha-\alpha_3)^2+\Delta^2]}\right]\\
&+4\chi_R^2\exp[-(\gamma_R+\alpha+\alpha_3)|\tau|]\\
&\times\left[\frac{\gamma_R^2\alpha}{[(\gamma_R-\alpha-\alpha_3)^2+\Delta^2][(\gamma_R-\alpha+\alpha_3)^2+\Delta^2][(\gamma_R+\alpha+\alpha_3)^2+\Delta^2]}\right]\\
&\times\{[(\gamma_R-\alpha)^2+\Delta^2-2\alpha_3(\gamma_R+\alpha)-3\alpha_3^2]\Delta\sin\Delta\tau\\
&\quad-[(\gamma_R-\alpha-\alpha_3)(\gamma_R-\alpha+\alpha_3)(\gamma_R+\alpha+\alpha_3)+\Delta^2(\gamma_R+\alpha+3\alpha_3)]\cos\Delta\tau\}\\
&+4\chi_R(\chi_M+\chi_T)\exp[-(\gamma_R+\alpha+\alpha_3)|\tau|]\left[\frac{\gamma_R\alpha}{[(\gamma_R+\alpha+\alpha_3)^2+\Delta^2][(\gamma_R-\alpha+\alpha_3)^2+\Delta^2]}\right]\\
&\times\{[(\gamma_R+\alpha+\alpha_3)(\gamma_R-\alpha+\alpha_3)-\Delta^2]\sin\Delta\tau+2\Delta(\gamma_R+\alpha_3)\cos\Delta\tau\}\ ,
\end{aligned}
\tag{7}
$$

and (ii) $\tau<0$,

$$
\begin{aligned}
I(\Delta,\tau)\propto{}&\chi_M^2\left[\frac{\gamma_M}{\gamma_M+2\alpha}\right]+\chi_T^2\left[\frac{\gamma_T}{\gamma_T+2\alpha}\right]+\chi_R^2\left[\frac{\gamma_R(\gamma_R+\alpha+\alpha_3)}{(\gamma_R+\alpha+\alpha_3)^2+\Delta^2}\right]\\
&+2\chi_M\chi_T\left[\frac{\gamma_M\gamma_T(\gamma_M+\gamma_T+4\alpha)}{(\gamma_M+\gamma_T)(\gamma_M+2\alpha)(\gamma_T+2\alpha)}\right]\\
&-2\chi_M\chi_R\left[\frac{\gamma_M\gamma_R\Delta}{(\gamma_M+\gamma_R+\alpha+\alpha_3)^2+\Delta^2}\right]\left[\frac{\gamma_M+2(\gamma_R+\alpha+\alpha_3)}{(\gamma_R+\alpha+\alpha_3)^2+\Delta^2}+\frac{1}{\gamma_M+2\alpha}\right]\\
&-2\chi_T\chi_R\left[\frac{\gamma_T\gamma_R\Delta}{(\gamma_T+\gamma_R+\alpha+\alpha_3)^2+\Delta^2}\right]\left[\frac{\gamma_T+2(\gamma_R+\alpha+\alpha_3)}{(\gamma_R+\alpha+\alpha_3)^2+\Delta^2}+\frac{1}{\gamma_T+2\alpha}\right]\\
&+\exp(-2\alpha|\tau|)\left[\chi_M^2+\chi_T^2+\chi_R^2\left[\frac{\gamma_R^2(\gamma_R+\alpha+\alpha_3)}{(\gamma_R+\alpha)[(\gamma_R+\alpha+\alpha_3)^2+\Delta^2]}\right]\right.\\
&\qquad\left.+2\chi_M\chi_T-2\chi_R(\chi_M+\chi_T)\left[\frac{\gamma_R\Delta}{(\gamma_R+\alpha+\alpha_3)^2+\Delta^2}\right]\right]\ .
\end{aligned}
\tag{8}
$$

Equations (7) and (8) are the main results of this section. In general, the RENFWM spectrum is different for τ and $-\tau$. However, as $|\tau|\rightarrow\infty$, Eq. (7) is identical to Eq. (8). Physically, when $|\tau|\rightarrow\infty$, beams 1 and 2 are mutually incoherent, therefore whether τ is positive or negative does not affect the RENFWM spectrum.

III. SUPPRESSION OF THERMAL BACKGROUND IN RENFWM SPECTRUM BY A TIME-DELAYED METHOD

The basic principle of the time-delayed method to suppress the thermal background is the following. Consider a nondegenerate FWM experiment with two pump beams (beams 1 and 2 in Fig. 1) coming from a single laser source and having the same polarization. The interference pattern of the pump beams will be in constant motion when the relative time delay between them is much longer than the laser coherence time. Now, we choose the laser linewidth such that $\gamma_M > \alpha \gg \gamma_T$. Because the phase of the interference pattern changes randomly on the scale of the laser coherence time, the integrated effect will wash out the thermal grating completely [7,18]. On the other hand, the molecular-reorientational grating has much shorter relaxation time. It will follow the randomly moved field interference pattern and therefore still exist [7]. In the Raman-enhanced nondegenerate four-wave mixing, the FWM signal has three origins, i.e., molecular reorientation, thermal effect, and Raman vibration. We are interested in the RENFWM spectrum. When $|\omega_1-\omega_3|$ equals the Raman-resonant frequency, the excitation of the Raman-active mode leads to a resonant structure in the spectrum. In contrast, the molecular-reorientational grating and the thermal grating give rise to a nonresonant background. When we increase the relative time delay between two pump beams, the nonresonant background decreases due to the elimination of the thermal background.

We consider the case that $\gamma_M, \gamma_R > \alpha \gg \gamma_T$. It can be shown from Eqs. (7) and (8) that under the condition $(\chi_T/\chi_M)^2(\gamma_T/2\alpha) \ll 1$, the thermal background can be eliminated completely when the relative time delay is much longer than the laser coherence time. In this limit, the theoretical RENFWM spectra show the normal asymmetry due to the interference between the Raman-resonant term and the nonresonant background originating solely from the molecular-reorientational grating. On the other hand, if $(\chi_T/\chi_M)^2(\gamma_T/2\alpha) \simeq 1$, the residue contribution from the thermal grating due to the second term in Eqs. (7) and (8) cannot be neglected even when $|\tau|\rightarrow\infty$. Our numerical results are given in Fig. 2. We normalize the signal intensity so that the maximum of the RENFWM signal equals one. Except the contribution from the thermal grating, all the parameters are the same in Figs. 2(a) and 2(b). For a typical sample, the relaxation time of the thermal grating is on the order of a microsecond, while the Debye relaxation time is only a few picoseconds, therefore it is reasonable to use the following parameters in the calculation: $\chi_M/\chi_R = 0.2$; $\gamma_M/\alpha = \gamma_R/\alpha = 10$; $\gamma_T/\alpha = 1\times10^{-5}$, and $\alpha_3/\alpha = 1$. In

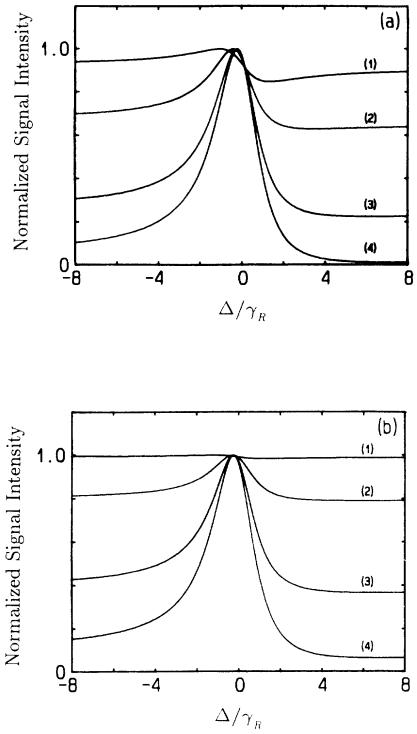

FIG. 2. Normalized RENFWM signal intensity vs Δ/γ_R for the different relative time delay. (a) $\chi_M/\chi_R = 0.2$; $\chi_T/\chi_R = 10$; $\gamma_M/\alpha = \gamma_R/\alpha = 10$; $\gamma_T/\alpha = 1\times10^{-5}$; $\alpha_3/\alpha = 1$ and (1) $\alpha\tau = 0$; (2) $\alpha\tau = 2$; (3) $\alpha\tau = 3$; (4) $\alpha\tau = 10$. (b) $\chi_M/\chi_R = 0.2$; $\chi_T/\chi_R = 100$; $\gamma_M/\alpha = \gamma_R/\alpha = 10$; $\gamma_T/\alpha = 1\times10^{-5}$; $\alpha_3/\alpha = 1$ and (1) $\alpha\tau = 0$; (2) $\alpha\tau = 4$; (3) $\alpha\tau = 5$; (4) $\alpha\tau = 10$.

contrast, we set $\chi_T/\chi_R = 10$ for Fig. 2(a) and $\chi_T/\chi_R = 100$ for Fig. 2(b). When $\alpha\tau = 0$, a huge nonresonant background originating from the thermal grating exists in the RENFWM spectrum, which obscures the Raman resonance signal almost completely in Fig. 2(b). However, the nonresonant background decreases drastically as $\alpha\tau$ increases. Since $(\chi_T/\chi_M)^2(\gamma_T/2\alpha) = 0.0125$ in Fig. 2(a), the signal from the thermal grating can be eliminated completely for sufficient time delay. At $\alpha\tau = 10$, the RENFWM spectrum in Fig. 2(a) converts to the corresponding RENFWM spectrum of a nonabsorbing sample, which has the same parameters except $\chi_T = 0$. On the other hand, because $(\chi_T/\chi_M)^2(\gamma_T/2\alpha) = 1.25$ in Fig. 2(b), the thermal grating always has a residue contribution to the nonresonant background even when $|\tau|\rightarrow\infty$. Here, we have given the results for $\alpha\tau > 0$ in Fig. 2. The basic features are the same for $\alpha\tau < 0$. In Appendix B, we give the analytical expressions of $I(\Delta,\tau)$ for the following case: $\alpha_3 = 0$, $\gamma_M, \gamma_R \gg \alpha \gg \gamma_T$, and $(\chi_T/\chi_M)^2(\gamma_T/2\alpha) \ll 1$.

We have demonstrated that if $(\chi_T/\chi_M)^2(\gamma_T/2\alpha) \ll 1$, the effect of the thermal grating on the RENFWM spectrum can be eliminated completely by a time-delayed method. In this case, the RENFWM spectrum of an absorbing and a nonabsorbing sample are identical in the limit of $|\tau|\rightarrow\infty$. Another interesting question is, for a

nonabsorbing sample, how the RENFWM spectrum depends on the time delay τ. By setting $\chi_T=0$ in Eqs. (7) and (8), we have, for $\gamma_M,\gamma_R \gg \alpha,\alpha_3$, the RENFWM spectrum is independent of τ. The τ dependence of the RENFWM spectrum becomes obvious when the laser linewidth increases. The numerical results are shown in Fig. 3. We note that Rahn, Farrow, and Lucht [19] and Agarwal and Farrow [20] have studied the time-delayed dependence of the CARS spectrum. They compared the difference between CARS spectrum at $\tau=0$ and $\tau\neq 0$ and found that the statistics of the pump beam plays an important role.

We have studied the time-delayed dependence of the RENFWM spectrum when pump beams (beams 1 and 2) are partially coherent light from a single laser source. Now, we consider the situation where pump beams are monochromatic light. In this case, beams 1 and 2 are always coherent even when $|\tau|\rightarrow\infty$. The variation of the relative time delay only changes the relative phase between them, hence the RENFWM spectrum should be independent of τ. By setting $\alpha=0$ in Eqs. (7) and (8) we have, for both $\tau>0$ and $\tau<0$,

$$I(\Delta,\tau)\propto\chi_M^2+\chi_T^2+\chi_R^2\left[\frac{\gamma_R(\gamma_R+\alpha_3)}{(\gamma_R+\alpha_3)^2+\Delta^2}\right]+2\chi_M\chi_T -2\chi_R(\chi_M+\chi_T)\left[\frac{\chi_R\Delta}{(\gamma_R+\alpha_3)^2+\Delta^2}\right], \quad (9)$$

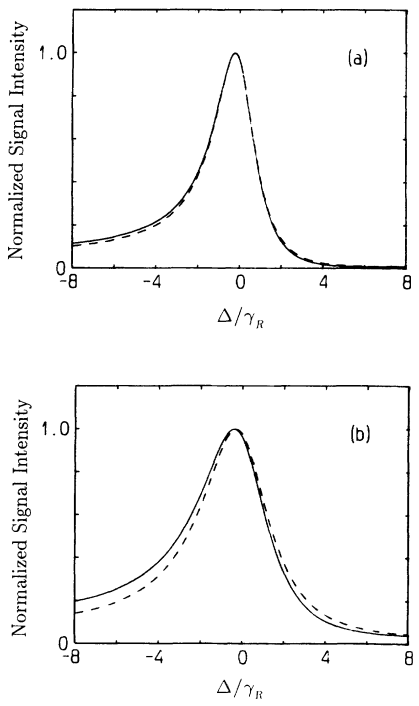

FIG. 3. Normalized RENFWM signal intensity vs Δ/γ_R in a nonabsorbing sample (i.e., $\chi_T/\chi_R=0$) for the different relative time delay. (a) $\chi_M/\chi_R=0.2$; $\gamma_M/\alpha=\gamma_R/\alpha=10$; $\alpha_3/\alpha=1$ and $\alpha\tau=0$ (solid line); $\alpha\tau=50$ (dashed line). (b) $\chi_M/\chi_R=0.2$; $\gamma_M/\alpha=\gamma_R/\alpha=2$; $\alpha_3/\alpha=1$ and $\alpha\tau=0$ (solid line); $\alpha\tau=50$ (dashed line).

which is independent of τ as we predict.

IV. DISCUSSION AND CONCLUSION

We have discussed the RENFWM spectrum at fixed time delay in the preceding section. Now, we turn our attention to the dependence of the RENFWM signal intensity on the relative time delay between beams 1 and 2 when the frequencies of the incident beams are fixed. Since this problem is closely related to the time-delayed coherent Raman spectroscopy with incoherent light [14], which is used to measure the ultrafast vibrational dephasing of the Raman mode, we restrict this discussion to the Raman term and neglect the contribution from the molecular-reorientational grating and the thermal grating (i.e., $\chi_M=\chi_T=0$).

Comparing Eqs. (7) and (8), it shows that when $\tau<0$, $I(\Delta,\tau)$ versus τ is only dependent on the coherence time of the pump beams. In contrast, both the laser coherence time and the relaxation time of the Raman mode affect the dependence of $I(\Delta,\tau)$ on τ when $\tau>0$. Physically, beam 1 is used to probe the Raman mode excited by beams 2 and 3. Therefore the Raman mode and beam 1 are mutually correlated only when beam 1 is delayed from beam 2 (i.e., $\tau>0$). Since the Raman mode decays with rate γ_R, $I(\Delta,\tau)$ versus τ depends on γ_R for $\tau>0$.

Figure 4 shows the logarithm of the RENFWM signal intensity versus $\gamma_R\tau$ at exact resonance ($\Delta=0$) and $\alpha_3=0$. The τ-independent background has been subtracted in the figure. As we predicted, the signal is asymmetric about $\tau=0$. When $\alpha\ll\gamma_R$, the temporal behavior of the RENFWM signal is mainly determined by the laser coherence time. The signal decays faster as α increases. In the limit of $\alpha\gg\gamma_R$, we have for $\tau>0$

$$I\propto 1+\left[\frac{\gamma_R}{\alpha}\right]\exp(-2\alpha|\tau|) -4\left[\frac{\gamma_R}{\alpha}\right]\exp[-(\gamma_R+\alpha)|\tau|] +4\left[\frac{\gamma_R}{\alpha}\right]\exp(-2\gamma_R|\tau|), \quad (10)$$

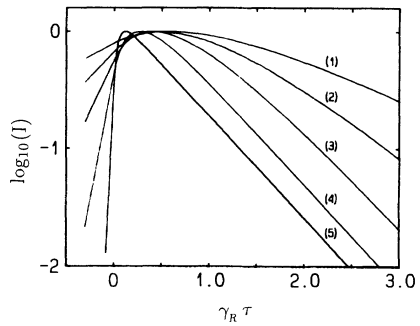

FIG. 4. Logarithm of the RENFWM signal intensity vs relative time delay $\gamma_R\tau$ at exact resonance ($\Delta/\alpha=0$) and $\alpha_3/\alpha=0$. The τ-independent background has been subtracted and the maximum of the signal is normalized to 1. (1) $\alpha/\gamma_R=0.5$; (2) $\alpha/\gamma_R=1$; (3) $\alpha/\gamma_R=2$; (4) $\alpha/\gamma_R=5$; (5) $\alpha/\gamma_R=20$.

and for $\tau<0$

$$I \propto 1+\left[\frac{\gamma_R}{\alpha}\right]\exp(-2\alpha|\tau|) . \tag{11}$$

Equation (10) shows that the RENFWM signal decays with decay rate $2\gamma_R$ at the tail of the signal ($\alpha\tau>1$), hence the dephasing time of the vibrational mode can be deduced. Furthermore, the comparison between Fig. 4 and Fig. 2 in Ref. [14] indicates that the coherent spike in the time-delayed RENFWM due to the autocorrelation function of the pump beams is smaller than in the time-delayed CSRS, which makes the measurement of γ_R easier in our case. We also note that, unlike the time-delayed CSRS, the maximum of the RENFWM signal does not occur at $\tau=0$. From Eq. (7), we obtain the delay time such that $I(0,\tau)$ is maximum for $\alpha_3=0$,

$$\tau_{\max}=\frac{1}{\alpha-\gamma_R}\ln\left[\frac{\gamma_R+\alpha}{2\gamma_R}\right] . \tag{12}$$

The α/γ_R dependence of $\gamma_R\tau_{\max}$ is given in Fig. 5. Another interesting thing in Eq. (7) is that when $\Delta\neq0$, $I(\Delta,\tau)$ exhibits damping oscillation for $\tau>0$. The amplitude of this oscillation increases as the linewidth of beam 2 increases. In Fig. 6, we show the logarithm of $I(\Delta,\tau)$ versus τ for the different frequency detuning Δ when $\alpha/\gamma_R=10$.

We have assumed that the laser sources are chaotic field in the above calculation. Chaotic field, which is used to describe a multimode laser source, is characterized by the fluctuation of both the amplitude and the phase of the field. Another commonly used stochastic model is the phase-diffusion model [15,16]. This model assumes that the amplitude of the laser field is a constant, while its phase diffuses as a random variable. Specifically, the dimensionless statistical factor in Eq. (1) can be written as $u(t)=\exp[i\phi(t)]$ and $u_3(t)=\exp[i\phi_3(t)]$ with $\langle\dot{\phi}(t)\dot{\phi}(t')\rangle=2\alpha\delta(t-t')$, $\langle\dot{\phi}_3(t)\dot{\phi}_3(t')\rangle=2\alpha_3\delta(t-t')$, and $\langle\dot{\phi}(t)\dot{\phi}_3(t')\rangle=0$. One interesting question is how the RENFWM signal behaves as the relative time delay between beams 1 and 2 varies if the laser sources are described by a phase-diffusion model.

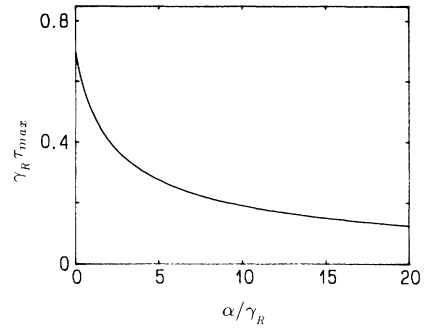

FIG. 5. $\gamma_R\tau_{\max}$ vs α/γ_R.

For the sake of simplicity, we consider the Raman term again and neglect the contribution from the molecular-reorientational grating and the thermal grating. By setting $\chi_M=\chi_T=0$ in Eq. (3), we have

$$I(\Delta,\tau)\propto(\chi_R\gamma_R)^2\int_0^\infty ds'\int_0^\infty dt'\langle u(t-\tau)u(t-s')u^*(t-\tau)u^*(t-t')\rangle \times\langle u_3(t-t')u_3^*(t-s')\rangle\exp[i\Delta(t'-s')]\exp[-\gamma_R(t'+s')] . \tag{13}$$

For the phase-diffusion model, the fourth-order coherence function is [16]

$$\langle u(t_1)u(t_2)u^*(t_3)u^*(t_4)\rangle=\exp[-\alpha(|t_1-t_3|+|t_1-t_4|+|t_2-t_3|+|t_2-t_4|)]\exp[\alpha(|t_1-t_2|+|t_3-t_4|)] . \tag{14}$$

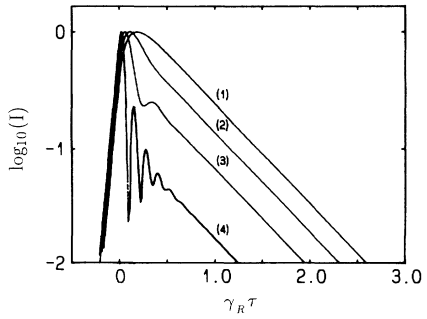

FIG. 6. Logarithm of the RENFWM signal intensity vs relative time delay $\gamma_R\tau$ for the off-resonant case with $\alpha/\gamma_R=10$ and $\alpha_3/\alpha=0$. The τ-independent background has been subtracted and the maximum of the signal is normalized to 1. (1) $\Delta/\alpha=0$; (2) $\Delta/\alpha=1$; (3) $\Delta/\alpha=2$; (4) $\Delta/\alpha=5$.

We have

$$\langle u(t-\tau)u(t-s')u^*(t-\tau)u^*(t-t')\rangle=\exp(-\alpha|t'-s'|) . \tag{15}$$

Also, if beam 3 has Lorentzian line shape, we have

$$\langle u_3(t-t')u_3^*(t-s')\rangle=\exp(-\alpha_3|t'-s'|) . \tag{16}$$

Substituting Eqs. (15) and (16) into (13), we obtain

$$I(\Delta,\tau)\propto\chi_R^2\frac{\gamma_R(\gamma_R+\alpha+\alpha_3)}{(\gamma_R+\alpha+\alpha_3)^2+\Delta^2} . \tag{17}$$

The above equation indicates that RENFWM is independent of τ, which is different completely from the result based on a chaotic model. The drastic difference of the results also exists in the other multiphoton processes

[21–24] when these two models are employed. Physically, the chaotic field has the property of photon bunching [25], which can affect any multiphoton process when the higher-order correlation function of the field plays an important role.

It is instructive to understand the temporal behavior of the RENFWM signal by a time-domain picture. In order to give a simple physical picture, we assume $\alpha_3=0$ and consider the Raman term at exact resonance (i.e., $\Delta=0$). We also restrict ourselves to the condition that $\alpha \gg \gamma_R$. This is the most interesting regime since it is closely related to the problem of the time-delayed FWM with incoherent light. According to Morita and Yajima [9], an incoherent light can be modeled as a sequence of square subpulses with pulse width $t_c=1/\alpha$. As shown in Fig. 7, subpulses are numbered and the corresponding subpulses of beams 1 and 2 are labeled by the same number. The electric field of subpulse n of beam 1 or 2 can be written as $f_n \exp[i(\mathbf{k}_i\cdot\mathbf{r}-\omega_1 t)]$ with $i=1,2$. For a phase-diffusion model, $f_n=f\exp(i\phi_n)$, with f a constant and ϕ_n a stochastic variable. On the other hand, both the amplitude and the phase fluctuate randomly for a chaotic field. If beam 1 is delayed from beam 2 by $\tau=Mt_c$, then subpulse 0 of beam 2 overlaps temporally with subpulse M of beam 1. Under the stationary condition, the induced polarization corresponding to Eq. (A9) is

$$P_R(\mathbf{r},t)=i(\chi_R\gamma_R)\varepsilon_3 \exp i[(\mathbf{k}_1-\mathbf{k}_2+\mathbf{k}_3)\cdot\mathbf{r}-\omega_3 t] \times \sum_{n=0}^{\infty} t_c f_M f_n^* \exp(-n\gamma_R t_c) , \tag{18}$$

or the signal intensity

$$I \propto \sum_{n=0}^{\infty} \langle |f_M|^2 |f_n|^2 \rangle \exp(-2n\gamma_R t_c) . \tag{19}$$

In the derivation of Eq. (19), we have used the relation $\langle |f_M|^2 f_n f_{n'}^* \rangle = 0$ for $n \neq n'$. Also, for $n \neq M$, we have

$$\langle |f_M|^2 |f_n|^2 \rangle = \langle |f_M|^2 \rangle \langle |f_n|^2 \rangle = (\langle |f_M|^2 \rangle)^2 .$$

For a phase-diffusion model, the field amplitude is a constant, therefore $\langle |f_M|^2 |f_n|^2 \rangle = |f|^4$ and

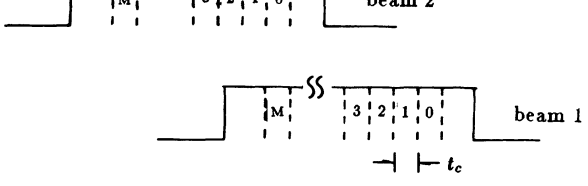

FIG. 7. Schematic diagram of the time-domain picture of the Raman-enhanced nondegenerate four-wave mixing. The incoherent lights of beams 1 and 2 are modeled as a sequence of square subpulses with pulse width $t_c=1/\alpha$. Subpulses are numbered, and the corresponding subpulses of beams 1 and 2 are labeled by the same number. Beam 1 is delayed from beam 2 by $\tau=Mt_c$, therefore subpulse 0 of beam 2 overlaps temporally with subpulse M of beam 1.

$$I \propto \sum_{n=0}^{\infty} \exp(-2n\gamma_R t_c) = \frac{1}{1-\exp(-2\gamma_R t_c)} . \tag{20}$$

In the limit of $\alpha \gg \gamma_R$, we have $I \propto \alpha/2\gamma_R$. Equation (20) indicates that the signal intensity is independent of the relative time delay if the incoherent light is characterized by a noisy phase and a stable amplitude. Now, let us consider a source with irregularities in its intensity distribution. In a nonlinear response proportional to higher-order correlation function of the field, the peaks in the irregularities are weighted more strongly than the valleys [22], therefore $\langle |f_M|^4 \rangle > (\langle |f_M|^2 \rangle)^2$. We have from Eq. (19)

$$I \propto 1+2\eta \left[\frac{\gamma_R}{\alpha}\right] \exp(-2\gamma_R \tau) , \tag{21}$$

with

$$\eta=[\langle |f_M|^4 \rangle - (\langle |f_M|^2 \rangle)^2]/(\langle |f_M|^2 \rangle)^2 .$$

For a chaotic source we have $\langle |f_M|^4 \rangle = 2(\langle |f_M|^2 \rangle)^2$, which leads to $\eta=1$. Besides a factor of two on the $\exp(-2\gamma_R\tau)$ term, Eq. (21) is consistent with Eq. (10) in the case of $\alpha\tau > 1$. The main purpose of the above discussion is that the time-domain picture reveals an important fact that the amplitude fluctuation of the incoherent light plays a critical role in the temporal behavior of the RENFWM signal. This is quite different from the time-delayed FWM with incoherent light in a two-level system [9], where T_2 of the system can be deduced. For the latter case, the phase fluctuation of the light is crucial.

In conclusion, we have studied theoretically the dependence of the RENFWM spectrum on the relative time delay between two pump beams when the thermal effect exists in the sample. Using the chaotic model for the incident laser beams, we give the conditions that the thermal background can be eliminated completely when the relative time delay is much longer than the laser coherence time. In this limit, the theoretical RENFWM spectra show the normal asymmetry due to the interference between the Raman-resonant term and the nonresonant background originating solely from the molecular-reorientational grating. We then turn our attention to the dependence of the RENFWM signal intensity on the relative time delay when the laser frequencies are fixed. Our results indicate that RENFWM is asymmetric about $\tau=0$ and the maximum of the RENFWM signal does not occur at $\tau=0$. When the beating frequency between the pump beam and the probe beam is off resonant from the Raman mode, the RENFWM signal exhibits damping oscillation as the time delay increases. We also show that the temporal behavior of the RENFWM signal is different drastically if the laser sources are described by a phase-diffusion model. The different roles of the phase fluctuation and the amplitude fluctuation can be understood by a time-domain picture.

ACKNOWLEDGMENTS

The authors gratefully acknowledge the financial support from the Chinese Academy of Sciences and the Chinese National Nature Sciences Foundation.

APPENDIX A

In this Appendix, we discuss the induced polarization originating from the molecular-reorientational grating, the thermal grating, and the Raman-active mode.

1. Molecular-reorientational grating

The order parameter $Q_M(\mathbf{r},t)$ of the molecular-reorientational grating induced by beams 1 and 2 satisfies the following equation [26]:

$$\frac{\partial Q_M}{\partial t}+\gamma_M Q_M=\frac{4}{3\nu}\Delta\alpha A_1 A_2^* , \tag{A1}$$

where $\gamma_M=5k_BT/\nu$ is the Debye relaxation rate, ν is a viscosity coefficient for an individual molecule, and $\Delta\alpha=\alpha_{\parallel}-\alpha_{\perp}$ is optical polarizability anisotropy. The formal solution of Eq. (A1) is

$$Q_M(\mathbf{r},t)=\frac{4\Delta\alpha}{3\nu}\int_0^{\infty}dt' A_1(\mathbf{r},t-t')A_2^*(\mathbf{r},t-t') \times\exp(-\gamma_M t') . \tag{A2}$$

The induced polarization which is responsible for the FWM signal is

$$\begin{aligned}P_M(\mathbf{r},t)&=\tfrac{2}{3}N\Delta\alpha Q_M(\mathbf{r},t)E_3(\mathbf{r},t)\\&=(\chi_M\gamma_M)\varepsilon_1\varepsilon_2^*\varepsilon_3\exp i[(\mathbf{k}_1-\mathbf{k}_2+\mathbf{k}_3)\cdot\mathbf{r}-\omega_3 t]\\&\quad\times\int_0^{\infty}dt' u_1(t-t')u_2^*(t-t')\\&\quad\times u_3(t)\exp(-\gamma_M t') ,\end{aligned} \tag{A3}$$

with $\chi_M=8N(\Delta\alpha)^2/9\nu\gamma_M$ and N the density of molecules.

2. Thermal grating

Consider the thermal grating established by beams 1 and 2. The variation in temperature through the sample $Q_T(\mathbf{r},t)$ obeys the diffusion equation [6]:

$$\frac{\partial Q_T}{\partial t}-D\nabla^2 Q_T=\frac{\zeta nc}{4\pi\rho C_p}A_1 A_2^* . \tag{A4}$$

Here, the diffusion constant $D=\beta/\rho C_p$; ρ, C_p, β, ζ, and n are the mass density, the specific heat per unit mass, the thermal conductivity, the loss of the medium, and the refractive index, respectively. We can solve Eq. (A4) formally, and obtain

$$Q_T(\mathbf{r},t)=\frac{\zeta nc}{4\pi\rho C_p}\int_0^{\infty}dt' A_1(\mathbf{r},t-t')A_2^*(\mathbf{r},t-t') \times\exp(-\gamma_T t') . \tag{A5}$$

Here, $\gamma_T=Dq_1^2$ is the relaxation rate of the thermal grating with $\mathbf{q}_1=\mathbf{k}_1-\mathbf{k}_2$. We have the nonlinear polarization created by the coupling between thermal grating and beam 3,

$$\begin{aligned}P_T(\mathbf{r},t)&=\frac{n}{2\pi}\left[\frac{\partial n}{\partial T}\right]_p Q_T(\mathbf{r},t)E_3(\mathbf{r},t)\\&=(\chi_T\gamma_T)\varepsilon_1\varepsilon_2^*\varepsilon_3\exp i[(\mathbf{k}_1-\mathbf{k}_2+\mathbf{k}_3)\cdot\mathbf{r}-\omega_3 t]\\&\quad\times\int_0^{\infty}dt' u_1(t-t')u_2^*(t-t')\\&\quad\times u_3(t)\exp(-\gamma_T t') ,\end{aligned} \tag{A6}$$

with $\chi_T=(\zeta n^2 c/8\pi^2\rho C_p\gamma_T)(\partial n/\partial T)_p$.

3. Excitation of the Raman-active mode

The beat between beams 2 and 3 will excite a Raman-active mode in the media with its normal coordinate $Q_R(\mathbf{r},t)$ satisfying [26]

$$\frac{\partial Q_R}{\partial t}+(\gamma_R-i\Delta)Q_R=\frac{i\alpha_R}{4\hbar}A_2^* A_3 . \tag{A7}$$

Here $\Delta=(\omega_1-\omega_3)-\omega_R$; ω_R and γ_R are the resonant frequency and the relaxation rate of the Raman mode, respectively. α_R is a parameter denoting the strength of the Raman interaction. The formal solution of Eq. (A7) is

$$Q_R(\mathbf{r},t)=\frac{i\alpha_R}{4\hbar}\int_0^{\infty}dt' A_2^*(\mathbf{r},t-t')A_3(\mathbf{r},t-t') \times\exp[-(\gamma_R-i\Delta)t'] . \tag{A8}$$

We have the nonlinear polarization responsible for the Raman-enhanced FWM signal,

$$\begin{aligned}P_R(\mathbf{r},t)&=\tfrac{1}{2}N\alpha_R Q_R(\mathbf{r},t)E_1(\mathbf{r},t)\exp[i(\omega_1-\omega_3)t]\\&=i(\chi_R\gamma_R)\varepsilon_1\varepsilon_2^*\varepsilon_3\exp i[(\mathbf{k}_1-\mathbf{k}_2+\mathbf{k}_3)\cdot\mathbf{r}-\omega_3 t]\\&\quad\times\int_0^{\infty}dt' u_1(t)u_2^*(t-t')u_3(t-t')\\&\quad\times\exp[-(\gamma_R-i\Delta)t'] ,\end{aligned} \tag{A9}$$

with $\chi_R=N\alpha_R^2/8\hbar\gamma_R$.

APPENDIX B

Consider the following case: $\alpha_3=0$, $\gamma_M,\gamma_R\gg\alpha\gg\gamma_T$, and $(\chi_T/\chi_M)^2(\gamma_T/2\alpha)\ll 1$. We obtain, from Eqs. (7) and (8), for (i) $\tau>0$,

$$I(\Delta,\tau)\propto\chi_M^2+\chi_R^2\left[\frac{\gamma_R^2}{\gamma_R^2+\Delta^2}\right]-2\chi_M\chi_R\left[\frac{\gamma_R\Delta}{\gamma_R^2+\Delta^2}\right]$$
$$+\exp(-2\alpha|\tau|)\left[\chi_M^2+\chi_T^2+\chi_R^2\left[\frac{\gamma_R^2}{\gamma_R^2+\Delta^2}\right]+2\chi_M\chi_T-2\chi_R(\chi_M+\chi_T)\left[\frac{\gamma_R\Delta}{\gamma_R^2+\Delta^2}\right]\right]$$
$$+4\chi_R^2\exp(-2\gamma_R|\tau|)\left[\frac{\gamma_R\alpha}{\gamma_R^2+\Delta^2}\right]^2$$
$$+4\chi_R\exp[-(\gamma_R+\alpha)|\tau|]\left[\frac{\gamma_R\alpha}{(\gamma_R^2+\Delta^2)^2}\right]$$
$$\times(\chi_R\gamma_R[\Delta\sin\Delta\tau-\gamma_R\cos\Delta\tau]+(\chi_M+\chi_T)[(\gamma_R^2-\Delta^2)\sin\Delta\tau+2\Delta\gamma_R\cos\Delta\tau]), \tag{B1}$$

and (ii) $\tau<0$,

$$I(\Delta,\tau)\propto\chi_M^2+\chi_R^2\left[\frac{\gamma_R^2}{\gamma_R^2+\Delta^2}\right]-2\chi_M\chi_R\left[\frac{\gamma_R\Delta}{\gamma_R^2+\Delta^2}\right]$$
$$+\exp(-2\alpha|\tau|)\left[\chi_M^2+\chi_T^2+\chi_R^2\left[\frac{\gamma_R^2}{\gamma_R^2+\Delta^2}\right]+2\chi_M\chi_T-2\chi_R(\chi_M+\chi_T)\left[\frac{\gamma_R\Delta}{\gamma_R^2+\Delta^2}\right]\right]. \tag{B2}$$

The above equations indicate that as $|\tau|\rightarrow\infty$, the signal from the thermal grating disappears completely and the RENFWM spectrum converts to the normal asymmetric structure originating from the interference between the Raman-resonant term and the nonresonant background. In this limit, the nonresonant background is solely due to the molecular-reorientational grating and the spectrum is independent of the laser linewidth.

[1] G. L. Eesley, *Coherent Raman Spectroscopy* (Pergamon, New York, 1981).
[2] M. D. Levenson, *Introduction to Nonlinear Laser Spectroscopy* (Academic, New York, 1982).
[3] P. D. Maker and R. W. Terhune, Phys. Rev. **137**, A801 (1965).
[4] D. Heiman, R. W. Hellwarth, M. D. Levenson, and G. Martin, Phys. Rev. Lett. **36**, 189 (1976).
[5] Z. Yu, H. Lu, P. Ye, and P. Fu, Opt. Commun. **61**, 287 (1987).
[6] G. Martin and R. W. Hellwarth, Appl. Phys. Lett. **34**, 371 (1979).
[7] P. Fu, Z. Yu, X. Mi, and P. Ye, J. Phys. (Paris) **48**, 2089 (1987).
[8] Z. Yu, X. Mi, Q. Jiang, P. Ye, and P. Fu, Opt. Lett. **13**, 117 (1988).
[9] N. Morita and T. Yajima, Phys. Rev. A **30**, 2525 (1984).
[10] S. Asaka, H. Nakatsuka, M. Fujiwara, and M. Matsuoka, Phys. Rev. A **29**, 2286 (1984).
[11] R. Beach, D. DeBeer, and S. R. Hartmann, Phys. Rev. A **32**, 3467 (1985).
[12] M. Fujiwara, R. Kuroda, and H. Nakatsuka, J. Opt. Soc. Am. B **2**, 1634 (1985).
[13] N. Morita, T. Tokizaki, and T. Yajima, J. Opt. Soc. Am. B **4**, 1269 (1987).
[14] T. Hattori, A. Terasaki, and T. Kobayashi, Phys. Rev. A **35**, 715 (1987).
[15] J. R. Klauder and E. C. G. Sudarshan, *Fundamentals of Quantum Optics* (Benjamin, New York, 1968), Chap. IX.
[16] B. Pincinbono and E. Boileau, J. Opt. Soc. Am. **58**, 784 (1967).
[17] J. W. Goodman, *Statistical Optics* (Wiley, New York, 1985).
[18] Z. Yu, X. Lu, X. Mi, Q. Jiang, and P. Fu, Opt. Commun. **85**, 63 (1991).
[19] L. A. Rahn, R. L. Farrow, and R. P. Lucht, Opt. Lett. **9**, 223 (1984).
[20] G. S. Agarwal and R. L. Farrow, J. Opt. Soc. Am. B **3**, 1596 (1986).
[21] L. Armstrong, Jr., P. Lambropoulos, and N. K. Rahman, Phys. Rev. Lett. **36**, 952 (1976).
[22] Y. R. Shen, Phys. Rev. **155**, 921 (1967).
[23] G. S. Agarwal, Phys. Rev. A **1**, 1445 (1970).
[24] C. Lecompte, G. Mainfray, C. Manus, and F. Sanchez, Phys. Rev. A **11**, 1009 (1975).
[25] R. Glauber, Phys. Rev. **131**, 2766 (1963).
[26] Y. R. Shen, *The Principles of Nonlinear Optics* (Wiley, New York, 1984).